

Spectral power and irradiance responsivity calibration of InSb working-standard radiometers

George Eppeldauer and Miklós Rác

New, improved-performance InSb power-irradiance meters have been developed and characterized to maintain the National Institute of Standards and Technology (NIST) spectral responsivity scale between 2 and 5.1 μm . The InSb radiometers were calibrated against the transfer-standard cryogenic bolometer that is tied to the primary-standard cryogenic radiometer of the NIST. The InSb radiometers serve as easy-to-use working standards for routine spectral power and irradiance responsivity calibrations. The spectral irradiance responsivities were derived from the spectral power responsivities by use of the measured area of the apertures in front of the InSb detectors. © 2000 Optical Society of America

OCIS codes: 040.0040, 040.3060, 040.5350, 120.5630, 230.5160.

1. Introduction

High-sensitivity infrared radiometer standards can eliminate signal-level problems caused by the weak outputs of commonly used thermal sources. An accurate infrared spectral responsivity scale has been realized for pyroelectric detectors at the National Physical Laboratory, UK.¹ The responsivity calibration of an InSb transfer standard detector has been reported for metrological applications from 1 to 3 μm .² The new infrared spectral responsivity scale developed at the National Institute of Standards and Technology (NIST) has been realized for a cryogenic bolometer³ that operates at much higher sensitivities (input power levels are 10 μW –20 pW) than pyroelectric detector-based scales (500–1 μW).

Working-standard InSb radiometers⁴ have been developed for the 2–5.1- μm wavelength range to maintain the spectral responsivity scale. These are easy to use compared with the sophisticated

cryogenic bolometer,⁵ which requires liquid-He sensor-temperature and continuous computer control monitors for corrections of responsivity changes.⁶ The design, characterization, and calibration of the spectral power responsivity of the improved-performance second-generation InSb radiometers are discussed in this paper. Realization of a new spectral irradiance responsivity scale is described also for the 2–5.1- μm wavelength range. Infrared test detectors with good uniformity of spatial response can be calibrated against the InSb working-standard radiometers in the radiant power measurement mode. Spatially nonuniform infrared detectors can be used for accurate radiometric measurements when they are calibrated against the working-standard InSb radiometers in the irradiance measurement mode.

2. Mechanical Structure of the InSb Radiometers

Following first-generation 4-mm-diameter InSb detectors,⁴ second-generation custom-made InSb radiometers have been developed at the EG&G Judson Company.⁷ Large-area and selected high-shunt-resistance detectors were mounted in 77-K Dewars. These InSb detectors were designed to minimize the problem of flashing⁴ even when they are exposed to short-wavelength optical radiation. Precision apertures of 6.4-mm diameter were mounted in all Dewars in front of the 7-mm-diameter InSb photovoltaic detectors. Long- and short-snout Dewars have been developed for different applications. In the long-snout version, shown

When this research was performed, G. Eppeldauer (geppeldauer@nist.gov) and M. Rác were with the Optical Technology Division, National Institute of Standards and Technology, Gaithersburg, Maryland 20899-3460. M. Rác was a guest researcher at the National Institute of Standards and Technology from the Hungarian Academy of Sciences Research Institute for Technical Physics and Materials Science, Budapest H-1121, Hungary. He is now with the Konkoly Observatory, Budapest H-1121, Hungary.

Received 27 April 2000; revised manuscript received 10 August 2000.

0003-6935/00/315739-06\$15.00/0

© 2000 Optical Society of America

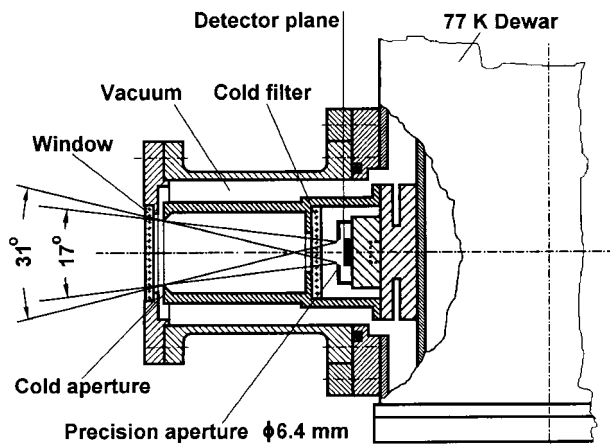


Fig. 1. Mechanical-optical construction of the second-generation (long-snout) InSb radiometer.

in Fig. 1, a 17° field-of-view (FOV) limiter was realized with a cold second aperture positioned 50 mm away from the precision aperture. The advantage of this arrangement is that laser beams can be measured if a wedged Dewar window is used to prevent interference and to produce a sufficient separation between the primary and the reflected beams in the plane of the precision aperture. Also, the background rejection is higher here than in the short-snout Dewar because of the 31° partial (clipped) FOV. The separation between the two apertures is only 7.2 mm in the short-snout Dewar. This unit is used only for measurements of noncoherent radiation for which easy alignment is an issue. The signal produced by the background is higher in the short-snout unit because of the 90° overall FOV (the unvignetted FOV remains 17°). Optical filters can be mounted inside the cylindrical holder of the cold FOV limiter. These radiometers can be used in both radiant power and irradiance measurement modes.

3. dc Background and ac Noise Test of the InSb Radiometers

The current-to-voltage converter gains of the InSb radiometers were designed to achieve a dc thermal-background-induced output voltage of less than 5 V.

An infrared collimator was used for ac noise tests. The infrared collimator was built from a variable-temperature blackbody (BB) radiator, a 25-cm-diameter reflecting (collimating) mirror, and a detector stage. An aperture wheel, a chopper, and then a shutter (this was the closest to the BB) were located in front of the BB cavity. The output voltage from the current-to-voltage converter of the InSb radiometer was measured with a lock-in amplifier.

The noise floor of the second-generation InSb radiometers was tested with a 40-Hz chopping frequency while the shutter was closed. From 10 measurements, a 6.7-pA standard deviation was calculated for the current noise of the broadband InSb-1 radiometer when the electrical bandwidth was 0.5 Hz. This value corresponds to that of a noise-equivalent photocurrent of 5 pA/Hz^{1/2}. The InSb-1 radiometer is a short-snout unit without any cold filter. This is our most frequently used working standard.

For high-sensitivity measurements, the background rejection of the long-snout InSb radiometer was further increased by installation of a cold filter (Model BBP-3200-3590-D, Spectrogon US, Inc.)⁷ with a bandpass of 3.2–3.6 μm (FWHM). The current-to-voltage gain could be increased from the 3 × 10⁴ V/A maximum of the short-snout unit to 10⁶ V/A where the dc background-induced output voltage was 1.6 V. A noise-equivalent power of 0.22 pW/Hz^{1/2} was obtained at the peak responsivity of the filtered InSb radiometer. The dynamic (signal) range was 6 orders of magnitude at the 10⁶-V/A gain.

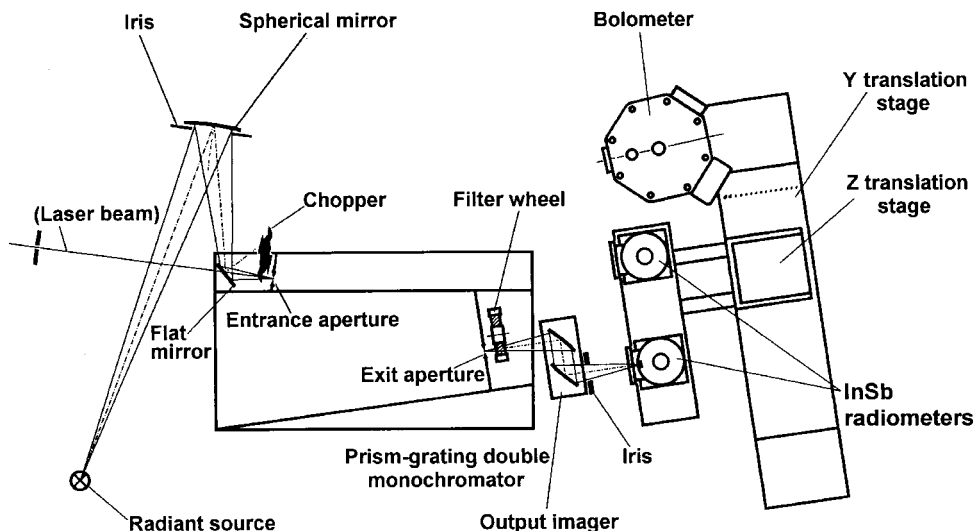


Fig. 2. Optical-mechanical scheme of the Ambient Infrared Spectral Comparator Facility.

4. Calibration Facility and Procedure

All measurements were performed at the NIST Ambient Infrared Spectral Comparator Facility.⁸ The optical-mechanical scheme of the facility is shown in Fig. 2.

The radiant sources were a 100-W tungsten halogen lamp from 2 to 3.65 μm and a 45-W ceramic glower from 3.65 to 5.7 μm . The sources were imaged onto the entrance aperture of the prism-grating double monochromator by spherical and flat mirrors. A chopper was positioned in front of the entrance aperture. Either 1- or 2-mm-diameter apertures could be used. An input iris was mounted upon the spherical mirror so that the solid angle of the beam entering the monochromator could be adjusted. The flat mirror was removable with a kinematic mount. The bandpass of the monochromator was $\sim 1\%$ of the selected wavelength. Laser beams could be introduced into the monochromator when the flat mirror was removed. The laser inputs were used either for wavelength calibration or to scan detectors with a small spot for high-resolution spatial response tests. Order-sorting filters were used at the exit aperture of the monochromator to improve the out-of-band blocking of the prism (KRS-5 crystal) predisperser of the monochromator. Off-axis paraboloid mirrors imaged the output beam to the detectors. The f/number of the output beam could be controlled with another iris. The detectors measured the total radiant power of the incident monochromatic beam (focused into a 2-mm-diameter spot on the detector surface) in underfilled mode. The kinematic mount of the bolometer was held by a separate stage, where it could be tilted, rotated, and shifted. Three InSb radiometers could be aligned on a second detector stage, which was mounted upon the computer-moved Z (vertical) translation stage. Both detector stages were mounted upon the computer-controlled Y (horizontal) translation stage.

Spatial response scans were made along the horizontal and vertical diameters of all detectors before we made measurements to determine the location of the beam spot in the center of the detector.

The calibration procedure included a number of spectral scans in different wavelength intervals. During a scan, the computer set the wavelength and moved the bolometer into the beam where the test points⁸ and the output signal were measured; then the first InSb radiometer was moved into the same beam, where its output signal was measured as well. During the responsivity scale derivation, a sufficient number of measured points and scans were selected to make the statistical evaluation easier. After all InSb radiometers were measured at a selected wavelength, the scan was repeated in 25- or 50-nm increments.

5. Measurement Results

Those electronic and radiometric characteristics of the second-generation InSb radiometers that could

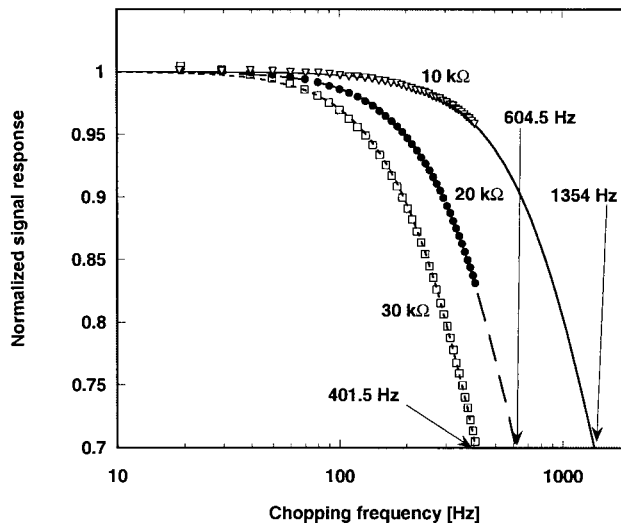


Fig. 3. Frequency-dependent signal responsivity curves of the InSb-1 radiometer at transimpedances of 10, 20, and 30 $\text{k}\Omega$.

influence the performance of the spectral responsivity calibrations were measured.

A. Frequency-Dependent Signal Responsivity

The frequency dependence of the InSb radiometer responsivity was measured to permit response corrections to be made for different chopping frequencies in different applications. Usually, dc signal responsivity is reported. The measured responsivity curves of the InSb-1 radiometer are shown in Fig. 3 at transimpedances of 10, 20, and 30 $\text{k}\Omega$. The 30- $\text{k}\Omega$ feedback resistor was used in the responsivity calibrations at the Ambient Infrared Spectral Comparator Facility. The lowest 3-dB roll-off frequency was ~ 400 Hz. The roll-off frequencies were determined from curve fits to a single time constant equivalent circuit of a low-pass RC filter.⁹ The chopping frequency (for a given application) should be selected to be 40 Hz or less to keep the operating point on the plateau of the responsivity curves.

B. Spatial Response

Horizontal and vertical scans were made through the detector centers with 2-mm-diameter beam spots. The purpose of these measurements was to check the spatial response uniformity of the detectors. We made the scans to find the plateau for power responsivity measurement and also to calculate an uncertainty component for the uncertainty budget. We avoided beam clipping by working in the center of the measured plateau.

Figure 4 shows the horizontal and vertical response scans of the InSb-1 radiometer. The response difference is shown for both scans relative to the response in the detector center. The scans appear to show that the degree of nonuniformity is 0.36% along a vertical diameter calculated as the standard deviation from seven points on the plateau. The nonuniformity along the perpendicular (horizon-

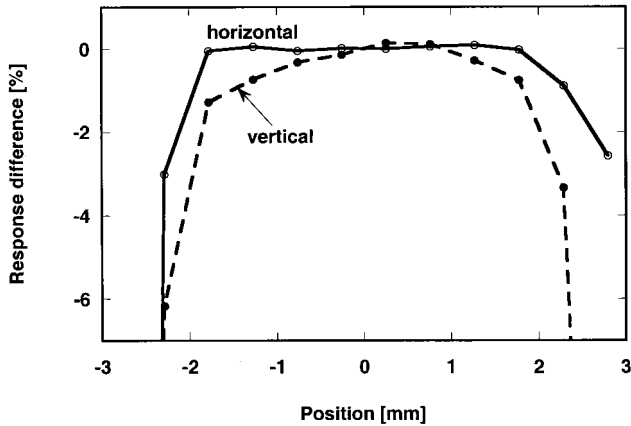


Fig. 4. Horizontal and vertical response scans of the InSb-1 radiometer. The curves show the response differences relative to the response in the detector center.

tal) diameter was much lower. The average run-to-run standard deviation for the seven points was 0.05%.

C. Spectral Power Responsivity

The measured spectral power responsivity curves of the second-generation InSb-1 and the first-generation InSb-0 radiometers are shown in Fig. 5. The curves were calculated from a number of spectral responsivity scans performed in a few-week period. The responsivity at each wavelength was determined from the average of at least four substitution measurements against the transfer-standard cryogenic bolometer. Both the transfer and the working standards were underfilled by the incident monochromatic radiation. The figure also shows the 100% external quantum efficiency¹⁰ (EQE; discussed below). The second-generation detector has improved

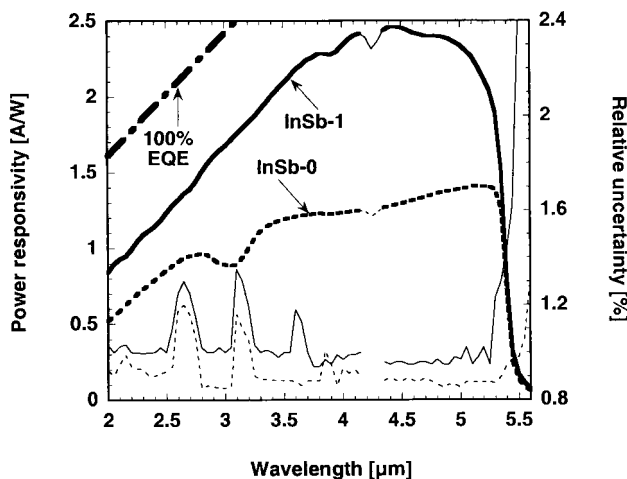


Fig. 5. Spectral responsivity curves of the first-generation (InSb-0) and second-generation (InSb-1) radiometers are shown. The responsivities measured at the 4.2- μm absorption band are shown where the curves become thinner. The theoretical limit of the responsivity is the 100% EQE curve. The two curves at the bottom are the uncertainties (scaled on the right-hand Y axis).

spectral responsivity. A roughly 5% dip at 4.2 μm and a smaller dip at 2.7 μm were caused by atmospheric absorption because the length of the optical path was different for the InSb detectors than for the transfer-standard bolometer. The dips at 4.2 μm are shown where the curves become thinner. Only the monochromator was purged. The other small dips at 3.2 μm were caused by absorption inside the InSb Dewars. We could obtain dip-free responsivity curves by either extending the purged beam passes or applying responsivity corrections. The right-side Y axis combines the relative uncertainties ($k = 1$) of the two-detector spectral responsivity measurements. Uncertainties are not shown for the 4.2- μm absorption band, for which high-accuracy calibrations are not suggested. Increased uncertainties can be seen at the other absorption bands. The low uncertainties reflect the small changes (drift) during a short substitution measurement at a selected wavelength. The uncertainties of the InSb-0 detector are fewer because of the better spatial response uniformity.

D. Spectral Irradiance Responsivity

We determined the spectral irradiance responsivity of the working-standard radiometers so we could calibrate test detectors with large spatial response non-uniformity. The response nonuniformities of these test detectors can be averaged out if they are calibrated in irradiance measurement mode for which both the standard and the test irradiance meters are overfilled with a uniform field of radiation.

The spectral irradiance responsivity of the standard meter is equal to the product of the spectral power responsivity and the area of the precision aperture in front of the detector. The second-generation InSb irradiance meters were built and used for two applications. In the first one, the broadband detector was utilized as a working standard in a short-snout Dewar. In the second application, we used a cold filter with a bandpass from 3.2 to 3.6 μm (FWHM) in a long-snout Dewar to measure the very low irradiance levels in the infrared collimator (mentioned in Section 3). We used this irradiance mode's working standard to calibrate the infrared collimator, and with it we also measured the area of small apertures (in the aperture wheel of the collimator) that are radiometrically relative to a large (mechanically measured) reference aperture. The details of the collimator calibration and its aperture area measurements are beyond the scope of this paper. The power levels measured on the collimator were lower than 0.1 mW where the detector nonlinearity was much less than 1%.^{2,4} At 10^6-V/A gain and 800 °C BB temperature, the signal-to-noise ratio of this irradiance meter was 2×10^3 when the smallest collimator aperture (0.2-mm diameter) was tested.

E. External Quantum Efficiency

The external quantum efficiency is $\text{EQE} = 1239.48 \times s/\lambda$, where s is the responsivity and λ is the wavelength. Also, $\text{EQE} = (1 - \rho) \times \text{IQE}$, where ρ is the

Table 1. Uncertainties of Power Responsivity Calibration with the Working-Standard InSb-1 Radiometer Outside the Atmospheric and Dewar Absorption Bands

Uncertainty Origin	Uncertainty ($k = 1$, %)	
	Type A ^a	Type B
Infrared spectral responsivity scale (on the bolometer) ^b		0.8
Bolometer spatial response nonuniformity		0.24
InSb-1 horizontal spatial response nonuniformity		0.05
InSb-1 vertical spatial response nonuniformity		0.36
Noise of the bolometer responsivity measurement	0.19	
Noise of the InSb-1 radiometer responsivity measurement	0.15	
Responsivity correction of the InSb-1 radiometer to 0 Hz		0.07
Bolometer preamplifier gain correction ^b		0.18
InSb-1 radiometer gain correction		0.07
Lock-in amplifier gain correction ^b		0.12
Bolometer responsivity corrections (temperature, bias, 3-dB roll-off measurements, and nonlinearity)	0.2	
InSb response nonlinearity ^c		0.1
Wavelength shift of the monochromator from 2 to 3.7 μm		0.3
Wavelength shift of the monochromator from 3.7 to 5.1 μm		0.1
Relative combined standard uncertainty from 2 to 3.7 μm		1.0
Relative combined standard uncertainty from 3.7 to 5.1 μm		0.95

^aRef. 11.

^bRef. 8.

^cRefs. 2 and 4.

reflectance and IQE is the internal quantum efficiency (equal to the ratio of the number of collected electrons to the number of photons absorbed by the detector). The EQE of the second-generation InSb detectors was almost twice that of the first-generation devices. The highest EQE (75%) was calculated at 3.6–3.7 μm for the InSb-1 detector. Both radiometer generations had sapphire windows with a transmittance of $\sim 90\%$ at 3 μm . The InSb-1 radiometer was equipped with a 1.8 μm cut-on (cold) filter. This filter has a transmittance of 90–95% for wavelengths longer than 2 μm . From the measured (and calculated) EQE and the signal loss caused by the window and the cold filter, a reflectance of $\sim 10\%$ can be estimated for the InSb-1 detector. The internal quantum efficiency is close to unity. The InSb-0 (first-generation) radiometer was not filtered.

6. Uncertainties

The uncertainties were evaluated and expressed according to the guidelines of NIST Technical Note 1297 (Ref. 11) and the standard ANSI/NCSS Z540-2-1997, “U.S. Guide to the Expression of Uncertainty in Measurement.”¹² The modeling of the measurement (the spectral power responsivity) and its measurement procedure have been discussed in detail in NIST Special Publication 250-42,⁸ where the uncertainty components were evaluated for determination of the spectral responsivity of the transfer-standard cryogenic bolometer.

In the present example, the power responsivity scale was derived from the cryogenic bolometer to the working-standard InSb-1 radiometer. The responsivity scale uncertainty of the bolometer dominates the uncertainty budget of the InSb working standard. The additional uncertainty sources of this scale derivation are summarized in Table 1. The uncertainty

components that contribute to the overall uncertainty are described below.

The uncertainty components caused by the spatial response nonuniformity of the bolometer and the InSb detector were calculated from spatial response scans as the standard deviation of the measured data points. All the data points utilized were located on the plateau of the response curves measured along the detector diameters, indicating that the incident beam was not clipped by the input optics of the radiometers. Because of the limitations in the vertical movement of the bolometer stage, only horizontal scans were made on the bolometer. The standard deviation from the horizontal scan represented the spatial response nonuniformity of the bolometer in the uncertainty budget.

The measurement noise was obtained from the standard deviation of the average responsivity. The InSb radiometer was substituted for the bolometer at least four times at each wavelength. Measurement noise includes the signal changes owing to component instabilities (e.g., source fluctuations) and wavelength-dependent (random) uncertainties of the monochromator. The long-term drift of the source did not produce any additional uncertainty component because the detector substitution at each wavelength took care of this problem. Also, the chopper duty factor (open-to-close ratio)-related uncertainty components could be neglected because the same chopper was used for both the bolometer and the InSb radiometer.

The frequency instability of the chopper produced an uncertainty component in the frequency-dependent responsivity corrections. The InSb radiometer’s responsivity correction was determined from the data fits of multiple 3-dB signal roll-off measurements at different photocurrent-to-voltage gains.

Table 2. Uncertainties of Irradiance Responsivity Calibration with the Working-Standard InSb-1 Radiometer

Uncertainty Origin	Uncertainty (%)	
	Type A	Type B
Power responsivity of the InSb-1 radiometer		1.00
Aperture area measurement of the InSb-1 radiometer		0.075
Directional responsivity of the InSb-1 radiometer within $f/4$	0.18	
Relative combined standard uncertainty ($k = 1$)		1.024

The photocurrent-to-voltage gains were measured against a standard current source (calibrator). The gain correction uncertainty includes the gain calibration uncertainty and the gain instabilities as well.

The uncertainty components that originate from the lock-in amplifier gain calibrations, the bolometer temperature, bias voltage, 3-dB roll-off frequency, and nonlinearity corrections were discussed in previous publications of Migdall and Eppeldauer.^{3,8} The uncertainty component caused by the InSb response nonlinearity was taken from previously published results for similar InSb detectors.^{2,4}

The uncertainty budget was determined for two wavelength ranges because the effect of the 5-nm maximum possible wavelength shift of the monochromator caused higher uncertainty from 2 to 3.7 μm compared with the uncertainty component from 3.7 to 5.1 μm . We have not specified any responsivity uncertainties at 4.2–4.3 μm . High-accuracy measurements should not be made (without purging) within this wavelength band where the atmospheric absorption is very high. All the uncertainty components in Table 1 are specified outside the absorption bands. The roughly 1% uncertainty components within the 2.7- and 3.2- μm absorption bands produced peaks in the combined uncertainties as shown in Fig. 5.

Table 2 is an extension of Table 1 for irradiance responsivity measurements with the same working-standard (InSb-1) radiometer. The aperture area was calculated from the average of several diameter measurements. The diameters were measured with a collimated beam geometry on an optical microscope. The aperture was positioned less than 1 mm away from the detector. The International Commission on Illumination (CIE)-recommended¹³ directional error $f_2(\epsilon)$ was calculated from directional (angular) response measurements of the InSb radiometer. $f_2(\epsilon)$ was less than 0.5% from -7° to 7° , which is roughly the angular range of the $f/4$ incident beam. The standard deviation of the directional responses within this angular range was 0.18%. This uncertainty component is used for unknown source distributions if the angular range of the source is within $f/4$.

7. Conclusion

High-electronic- and radiometric-performance InSb radiometers have been developed, characterized, and calibrated to maintain the spectral power and irradiance responsivity scales from 2 to 5.1 μm . The relative uncertainty ($k = 1$) of the responsivity scales

maintained by the working-standard radiometers is $\sim 1\%$. Test infrared radiometers can be calibrated against the working-standard InSb radiometers in both power and irradiance measurement modes.

References and Notes

1. D. H. Nettleton, T. R. Prior, and T. H. Ward, "Improved spectral responsivity scales at the NPL, 400 nm to 20 μm ," *Metrologia* **30**, 425–432 (1993).
2. L.-P. Boivin, "Properties of indium antimonide detectors for use as transfer standards for detector calibrations," *Appl. Opt.* **37**, 1924–1929 (1998).
3. A. Migdall and G. Eppeldauer, "Realization of an infrared spectral radiant power response scale on a cryogenic bolometer," *Metrologia* **35**, 307–315 (1998).
4. G. P. Eppeldauer, A. L. Migdall, and L. M. Hanssen, "InSb working standard radiometers," *Metrologia* **35**, 485–490 (1998).
5. G. Eppeldauer, A. L. Migdall, and C. L. Cromer, "A cryogenic silicon resistance bolometer for use as an infrared transfer standard detector," in *Thermal Phenomena at Molecular and in Cryogenic Infrared Detectors*, M. Kaviany, D. A. Kaminski, A. Majumdar, P. E. Phelan, M. M. Yovanovich, and Z. M. Zhang, eds., book H00908-1994 (American Society of Mechanical Engineers, New York), pp. 63–67.
6. G. Eppeldauer, A. L. Migdall, T. R. Gentile, and C. L. Cromer, "Absolute response calibration of a transfer standard cryogenic bolometer," in *Photodetectors and Power Meters II*, K. Muray and K. J. Kaufmann, eds., *Proc. SPIE* **2550**, 36–46 (1995).
7. Identification of commercial equipment to specify adequately an experimental problem does not imply recommendation or endorsement by the NIST, nor does it imply that the equipment identified is necessarily the best available for the purpose.
8. A. L. Migdall and G. P. Eppeldauer, *Spectroradiometric Detector Measurements. III. Infrared Detectors*, Natl. Inst. Stand. Technol. Spec. Publ. 250-42 (U.S. Government Printing Office, Washington, D.C., 1998).
9. G. P. Eppeldauer, "Noise-optimized silicon radiometers," *J. Res. Natl. Inst. Stand. Technol.* **105**, 209–219 (2000).
10. T. C. Larason, S. S. Bruce, and A. C. Parr, *Spectroradiometric Detector Measurements. I. Ultraviolet Detectors; II. Visible and Near-Infrared Detectors*, Natl. Inst. Stand. Technol. Spec. Publ. 250-41 (U.S. Government Printing Office, Washington, D.C., 1998), p. 35.
11. B. N. Taylor and C. E. Kuyatt, *Guidelines for Evaluating and Expressing the Uncertainty of NIST Measurement Results*, Natl. Inst. Stand. Technol. Tech. Note 1297 (U.S. Government Printing Office, Washington, D.C., 1994).
12. American National Standards Institute/National Conference of Standards Laboratories, "American National Standard for Expressing Uncertainty—U.S. Guide to the Expression of Uncertainty in Measurement," ANSI/NCSL Z540–2-1997 (National Conference of Standards Laboratories, Boulder, Colo., 1998).
13. Commission International d'Eclairage, "Methods of characterizing the performance of radiometers and photometers," CIE Publ. No. 53 (TC-2.2) (CIE, Vienna, Austria, 1982).